Cell Reports

CaMKK2 Regulates Mechanosensitive Assembly of Contractile Actin Stress Fibers

Graphical Abstract
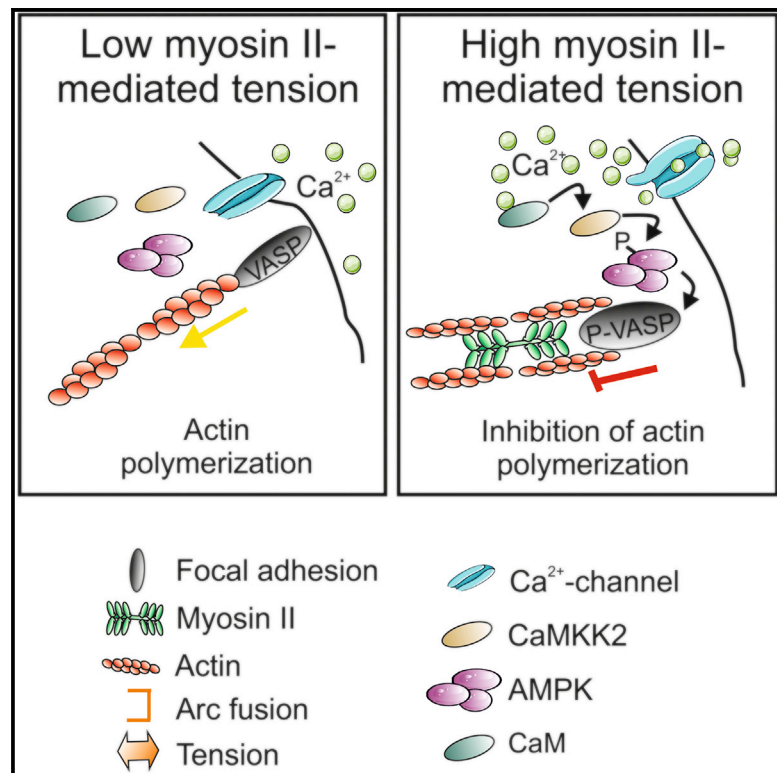
Authors

Sari Tojkander, Katarzyna Ciuba,
Pekka Lappalainen

Correspondence

sari.tojkander@helsinki.fi

In Brief

Contractile actomyosin bundles control cell morphology, adhesion, and migration. Tojkander et al. show that the maturation of actomyosin bundles occurs through activation of local, mechanosensitive Ca^{2+} influx that triggers CaMKK2/AMPK-dependent signaling cascade at focal adhesions.

Highlights

- Local Ca^{2+} influxes activate CaMKK2 at focal adhesions

- CaMKK2 is critical for mechanosensitive AMPK phosphorylation at focal adhesions

- Inhibition of CaMKK2 prevents maturation of contractile actomyosin bundles

CellPress

Report

CaMKK2 Regulates Mechanosensitive Assembly of Contractile Actin Stress Fibers

Sari Tojkander,[1,3,*] Katarzyna Ciuba,[2] and Pekka Lappalainen[2]
[1]Section of Pathology, Department of Veterinary Biosciences, University of Helsinki, Helsinki, Finland
[2]Institute of Biotechnology, University of Helsinki, Helsinki, Finland
[3]Lead Contact
*Correspondence: sari.tojkander@helsinki.fi
https://doi.org/10.1016/j.celrep.2018.06.011

SUMMARY

Stress fibers are contractile actomyosin bundles that guide cell adhesion, migration, and morphogenesis. Their assembly and alignment are under precise mechanosensitive control. Thus, stress fiber networks undergo rapid modification in response to changes in biophysical properties of the cell's surroundings. Stress fiber maturation requires mechanosensitive activation of 5′AMP-activated protein kinase (AMPK), which phosphorylates vasodilator-stimulated phosphoprotein (VASP) to inhibit actin polymerization at focal adhesions. Here, we identify Ca^{2+}-calmodulin-dependent kinase kinase 2 (CaMKK2) as a critical upstream factor controlling mechanosensitive AMPK activation. CaMKK2 and Ca^{2+} influxes were enriched around focal adhesions at the ends of contractile stress fibers. Inhibition of either CaMKK2 or mechanosensitive Ca^{2+} channels led to defects in phosphorylation of AMPK and VASP, resulting in a loss of contractile bundles and a decrease in cell-exerted forces. These data provide evidence that Ca^{2+}, CaMKK2, AMPK, and VASP form a mechanosensitive signaling cascade at focal adhesions that is critical for stress fiber assembly.

INTRODUCTION

Stress fibers are the most prominent force-producing actomyosin structures in many non-muscle cells, where they contribute to adhesion, migration, and mechanotransduction (Tojkander et al., 2012; Burridge and Wittchen, 2013; Kassianidou and Kumar, 2015). Stress fibers can be divided into three subgroups based on their protein compositions and associations with focal adhesions (Small et al., 1998, Naumanen et al., 2008). "Dorsal stress fibers" are non-contractile actin filament bundles that elongate toward the cell center through VASP and formin-driven actin filament polymerization at focal adhesions located at their distal ends (Watanabe et al., 1999; Hotulainen and Lappalainen, 2006; Tojkander et al., 2011, 2015; Oakes et al., 2012; Tee et al., 2015). "Transverse arcs" are thin actin filament bundles composed of a periodic α-actinin-myosin II pattern. They form

parallel to the leading edge and undergo retrograde flow toward the cell center in connection with the elongating dorsal stress fibers (Hotulainen and Lappalainen, 2006; Burnette et al., 2011, 2014; Tojkander et al., 2011). As the transverse arcs flow toward the cell center, they fuse with each other to form thicker actomyosin bundles that exert strong traction forces to the focal adhesions that are linked, through dorsal stress fibers, to their ends. This leads to a formation of a thick, straight actomyosin bundle ("ventral stress fiber"), which is anchored to focal adhesions from its both ends (Hotulainen and Lappalainen, 2006; Tojkander et al., 2015; Soiné et al., 2015). Ventral stress fibers represent the major force-generating actomyosin bundles in migrating cells.

Stress fiber assembly is regulated by several signaling cascades, of which the RhoA pathway is the best characterized so far (Ridley and Hall 1994; Chrzanowska-Wodnicka and Burridge, 1996; Ridley, 2015). In addition to biochemical signaling cascades, stress fiber assembly is controlled by mechanosensitive pathways. This is because ventral stress fibers are present only in cells grown on stiff matrices, and their assembly and alignment can be controlled through applying external forces to cells (Discher et al., 2005; Prager-Khoutorsky et al., 2011). On the other hand, dorsal stress fibers and transverse arcs are also present in cells growing on a soft environment, indicating that the maturation of ventral stress fibers from their precursors is the mechanosensitive phase of the process (Tojkander et al., 2015). Previous studies revealed that increased myosin-II-mediated contractility during the lateral fusion of transverse arcs activates a tension-sensitive signaling cascade in focal adhesions that is critical for maturation of ventral stress fibers. In this process, mechanosensitive AMPK-mediated phosphorylation of actin filament assembly factor VASP inhibits vectorial actin polymerization at focal adhesions connected to the ends of ventral stress fibers. Consequently, elongation of the ventral stress fiber is halted, thus ensuring proper contractility of the actomyosin bundle (Tojkander et al., 2015). However, the upstream components of the mechanosensitive AMPK-dependent pathway have remained unknown.

AMPK has been mainly linked to the regulation of central metabolic pathways (Bonini and Gantner, 2013). Several lines of evidence show that Lkb1 is the main upstream kinase of AMPK in metabolic stress, although other kinases are required for AMPK function in response to different cellular stimuli (Hawley et al., 2003; Shaw et al., 2004; Altarejos et al., 2005; Hurley et al., 2005). The best characterized of these other AMPK kinases is CaMKK2, which activates AMPK both *in vitro* as well as in different cell lines and organisms (Hong et al., 2005; Hurley

et al., 2005; Woods et al., 2005). CaMKK2 can be activated through elevation of cytoplasmic Ca^{2+} concentration in response to hormones and metabolites (Marcelo et al., 2016), and it phosphorylates AMPK in a Ca^{2+}-dependent manner also in the absence of Lkb1 (Hawley et al., 2005). Because CaMKK2-dependent AMPK activation was also linked to exercise-mediated tension in skeletal muscle cells (Jensen et al., 2007; Abbott et al., 2009), we studied here the possible role of CaMKK2 in mechanosensitive activation of AMPK in focal adhesions of non-muscle cells.

RESULTS

Compromised CaMKK2 Activity Leads to Loss of Mature Actomyosin Bundles and Decreased Cell-Mediated Forces

To examine whether CaMKK2 is involved in the mechanosensitive stress fiber maturation, we utilized CaMKK2 small interfering RNA (siRNA) and a CaMKK2 inhibitor, STO-609 (Tokumitsu et al., 2002), to diminish the activity of this kinase in U2OS cells. CaMKK2 knockdown cells and the cells treated with a CaMKK2 inhibitor displayed abnormal stress fiber phenotype, characterized by long dorsal stress fibers and lack of thick ventral stress fibers (Figures 1A, S1A–S1C, and S1E–S1G; Video S1). This phenotype is similar to the one of cells, in which VASP phosphorylation was diminished through inhibition of AMPK (Tojkander et al., 2015).

The remaining stress fibers in CaMKK2-depleted cells were less contractile compared to control cells, as analyzed from cells grown on crossbow-shaped patterns (Figures 1B, 1C, and S1H). Moreover, traction force microscopy revealed that CaMKK2 knockdown cells, and the cells treated with a CaMKK2 inhibitor, displayed defects in exerting traction forces to the substratum and a decrease in the contractile moment (Figures 1D–1F and S1I). Also, exogenous expression of a G87R CaMKK2 mutant, which behaves as a dominant-negative inhibitor of CaMKK2 signaling (O'Brien et al., 2017), led to immature stress fiber network (Figure S2A). Thus, CaMKK2 activity is critical for the maturation of force-producing ventral stress fibers.

CaMKK2 Contributes to Stress Fiber Maturation by Regulating AMPK-Mediated Phosphorylation of VASP

Because inhibition of CaMKK2 led to a stress fiber phenotype that resembled AMPK-deficient cells and cells overexpressing constitutive active VASP, we examined whether CaMKK2 regulates stress fiber assembly and contractility through the AMPK-VASP pathway. Phosphorylation of AMPK at Thr172 is indicative of its activation, and phosphorylation of VASP at the AMPK target site Ser239 inhibits its actin polymerization activity (Benz et al., 2009). We thus examined the levels of P-Thr172-AMPK and P-Ser239-VASP in lysates of U2OS cells treated with CaMKK2 inhibitor, STO-609, and in CaMKK2 siRNA knockdown cells. In all cases, CaMKK2-deficient cells exhibited significantly lower levels of phosphorylated AMPK and phosphorylated VASP compared to control cells, and the total protein levels of AMPK and VASP remained unchanged (Figures 2A–2D and S2B).

Phosphorylation of VASP on Ser239 is regulated in a tension-dependent manner, and this is essential for the maturation of force-producing actomyosin bundles (Tojkander et al., 2015). Thus, we studied whether CaMKK2 activity is critical for cell-exerted forces and VASP phosphorylation in cells cultured on different rigidities. CaMKK2 inhibitor-treated U2OS cells, cultured on 26-kPa matrix, displayed lower traction forces compared to the control cells, and exposure to this inhibitor on cells plated on a soft (4-kPa) matrix did not affect the root-mean-square tractions (Figures 2E and 2F). Moreover, cells grown on rigid substratum (glass) displayed diminished levels of phosphorylated AMPK and VASP in response to inhibition of CaMKK2. However, on a soft matrix (2 kPa), the effect of CaMKK2 inhibition on the levels of phosphorylated AMPK and VASP was negligible (Figures S2C and S2D). These data provide evidence that CaMKK2 is critical for mechanosensitive phosphorylation of AMPK and VASP.

CaMKK2-AMPK-VASP Pathway Is Activated by Ca^{2+} Influx at Focal Adhesions

Because VASP-driven stress fiber elongation occurs predominantly in focal adhesions (Tojkander et al., 2015), we examined whether CaMKK2 and AMPK localize to focal adhesions in migrating U2OS cells. In addition to diffusing cytoplasmic localization, endogenous CaMKK2 accumulated to the tips of ventral stress fibers (Figures 3A and 3C). Moreover, exogenously expressed CaMKK2-flag protein was enriched at focal adhesions located at the tips of ventral stress fibers (Figures 3B and 3D). Finally, Thr172-phosphorylated, active form of AMPK displayed enrichment to focal adhesions (Figure S3A).

CaMKK2 can be activated through Ca^{2+} influxes, and this is essential for its ability to phosphorylate AMPK (Racioppi and Means, 2012). To examine whether Ca^{2+} influxes occur at focal adhesions, U2OS cells were transfected with a plasmid expressing mCherry-fusion of a focal adhesion protein zyxin and a Ca^{2+} indicator GCaMP6. Total internal reflection microscopy (TIRF) analysis revealed elevated Ca^{2+} levels at zyxin-positive foci (Figure 3E). Importantly, the Ca^{2+} levels were higher at the ends of contractile ventral stress fibers as compared to non-contractile dorsal stress fibers (Figures 3F, S3B, and S3C). To examine the mechanosensitivity of Ca^{2+} influxes, we utilized blebbistatin to inhibit myosin II. Cells treated with 10 μM blebbistatin started to lose specific GCaMP6 signal at the ends of contractile actomyosin bundles few minutes following blebbistatin administration (Figures 3G and 3H). Moreover, cells grown on compliant matrix (4 kPa polyacrylamide gel) that do not contain mature ventral stress fibers did not display detectable Ca^{2+} enrichment at the ends of remaining (non-contractile) dorsal stress fibers (Figure S3D). Thus, proper contractility of ventral stress fibers appears to be crucial for inducing Ca^{2+} influxes in focal adhesions located at their ends.

To assess the possible role of Ca^{2+} influxes in stress fiber maturation, we first cultured U2OS cells in a Ca^{2+}-free medium. Three-hour incubation in a Ca^{2+}-free medium resulted in a similar disappearance of thick ventral stress fibers as inhibition of CaMKK2 or AMPK or culturing the cells on soft matrix (Figures S4A–S4D). To more specifically examine the role of mechanosensitive Ca^{2+} channels in this process, we utilized GsMTx-4, a
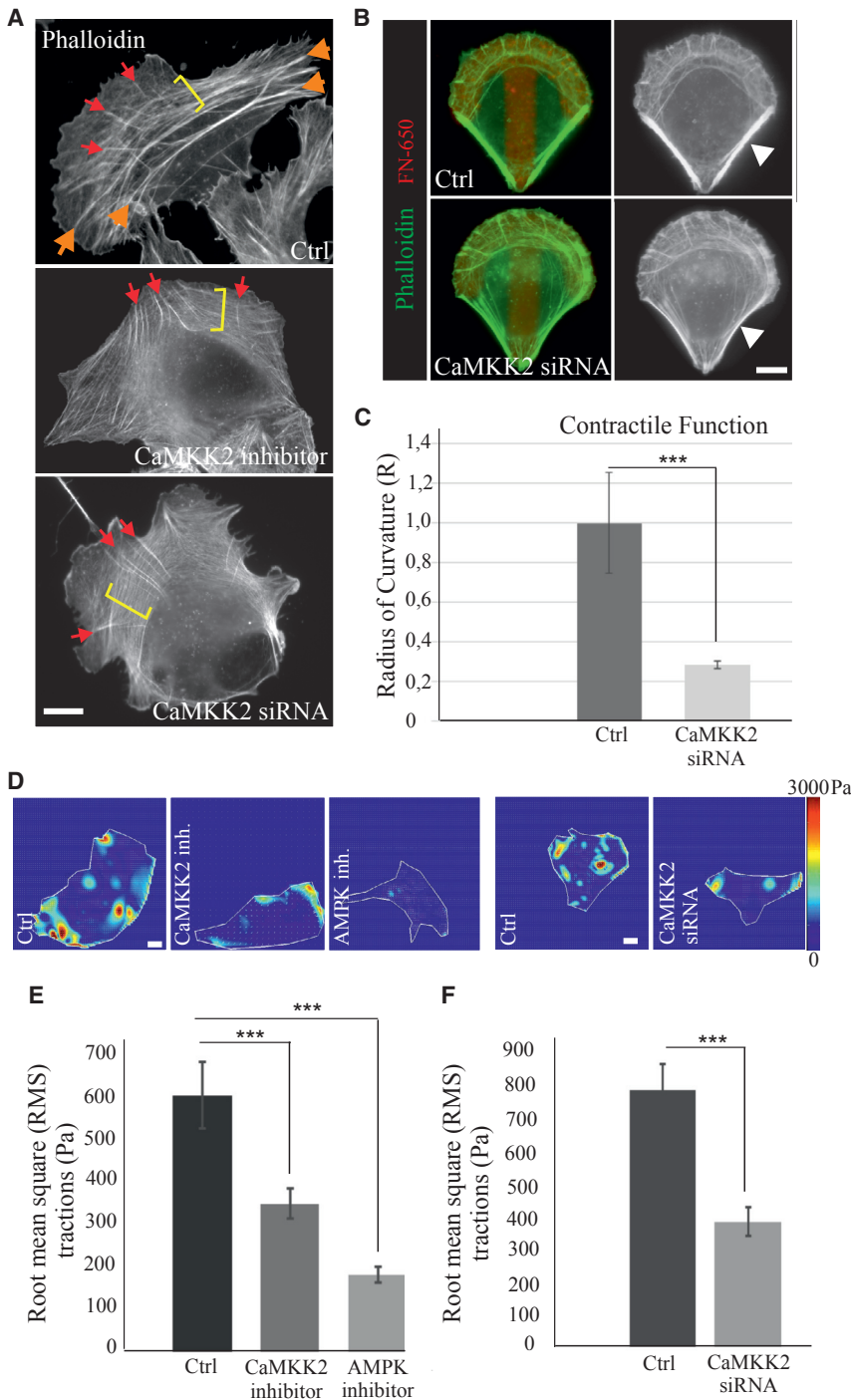
Figure 1. Compromised CaMKK2 Activity Leads to Loss of Contractile Ventral Stress Fibers and Subsequent Decrease in Cell-Mediated Forces

(A) Stress fiber phenotypes of U2OS cells treated with CaMKK2 inhibitor (5 μM STO-609 in DMSO) or CaMKK2-specific siRNA. Control cells were treated with DMSO and scrambled siRNA, respectively. Visualization of F-actin by phalloidin staining revealed almost complete loss of thick ventral stress fibers in cells lacking active CaMKK2. Red arrows, dorsal stress fibers; yellow brackets, transverse arcs; orange arrow, ventral stress fiber. The scale bar represents 10 μm.

(B) Representative control (Ctrl) and CaMKK2-depleted U2OS cells grown on crossbow-shaped fibronectin-650-coated micropatterns and stained with Alexa 488-phalloidin. Arrowheads indicate the contractile ventral stress fibers. Curvature of the bundle is indicative of lower contractile function. The scale bar represents 10 μm.

(C) Based on the calculated radius of curvature (for details, see Figure S1H), the ventral stress fibers of CaMKK2-depleted cells grown on micropatterns were ~3-fold less contractile compared to the control cells. Mean (±SEM) is shown; n = 59 for both control and CaMKK2 knockdown cells. Values obtained from control cells were normalized to 1; ***p < 0.001 (Mann-Whitney-Wilcoxon rank-sum test).

(D) Representative traction force maps of control (DMSO), CaMKK2 inhibitor (STO-609 5 μM in DMSO), AMPK inhibitor (compound C 5 μM in DMSO), control siRNA, and CaMKK2-siRNA-treated cells. The scale bars represent 10 μm.

(E) Quantification of cell-exerted traction forces of control, CaMKK2-inhibited, and AMPK-inhibited cells. Mean (±SEM) is shown; n(ctrl) = 77; n(STO-609) = 44; n(CmpdC) = 21; ***p < 0.001 (Mann-Whitney-Wilcoxon rank-sum test).

(F) Quantification of cell-exerted traction forces of U2OS cells treated with control or CaMKK2 siRNA oligonucleotides. Mean (±SEM) is shown; n(ctrl siRNA) = 34; n(CaMKKII siRNA) = 26; ***p < 0.001 (Mann-Whitney-Wilcoxon rank-sum test).

compound that inhibits several tension-sensitive TRP family as well as piezo ion channels (Sugimoto et al., 2017). Administration of 5 μM GsMTx-4 to sparse U2OS cell cultures led to appearance of an immature stress fiber network, characterized by long dorsal stress fibers, arrays of thin transverse arcs, and lack of thick ventral stress fibers (Figures 4A and 4B). Cells treated with 5 μM GsMTx-4 displayed also lower levels of P-Thr172-AMPK and P-Ser239-VASP (Figures 4C and 4D). Reciprocally, treatment of cells with Ca²⁺ ionophore resulted in an increase in the levels of P-Ser239-VASP (Figures S4E and S4F). Together, these results suggest that local Ca²⁺ influxes through mechanosensitive ion channels activate the CaMKK2-AMPK pathway to catalyze the inhibitory phosphorylation of actin polymerization factor VASP at the ends of contractile ventral stress fibers.

DISCUSSION

AMPK has a well-established role in metabolic processes as a key sensor of cellular energy status. AMPK is activated upon
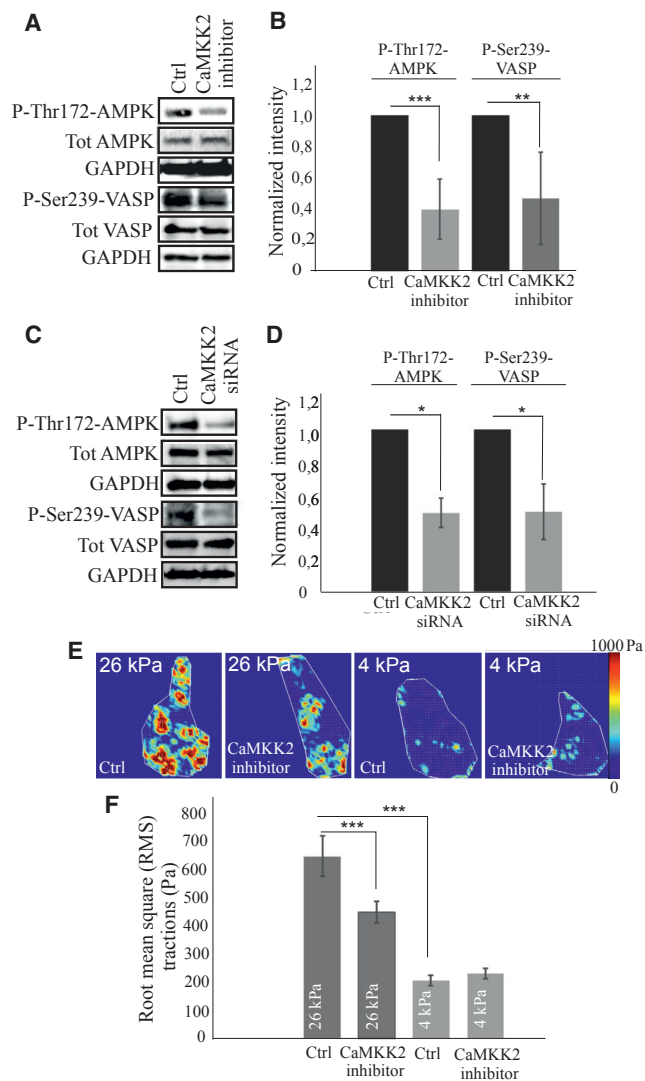
Figure 2. CaMKK2 Is Critical for Mechanosensitive Phosphorylation of AMPK and VASP

(A) P-Thr-172-AMPK, P-Ser239-VASP, as well as total AMPK and VASP were detected from the lysates of control (DMSO) and CaMKK2 inhibitor (5 μM STO-609 in DMSO)-treated U2OS cells by western blotting. GAPDH was used as a loading control.

(B) Quantification of P-Thr172-AMPK and P-Ser239-VASP levels (compared to total VASP/AMPK) from control and CaMKK2-inhibited cells. Intensity values of phosphorylated proteins were divided by the intensity values of total protein. The obtained intensity value from control cells was set to 1. Mean (±SD) is shown; n(P-Thr172-AMPK) = 5 and n(P-Ser239-VASP) = 6; ***p < 0.001; **p < 0.01 (paired t test).

(C) P-Thr-172-AMPK, P-Ser239-VASP, as well as total AMPK and VASP were detected from control siRNA and CaMKK2 siRNA cell lysates cell by western blotting. GAPDH was used as a loading control.

(D) Quantification of P-Thr172-AMPK and P-Ser239-VASP levels (compared to total VASP/AMPK) from control and CaMKK2 knockdown cells. Intensity values of phosphorylated proteins were divided by the intensity values of total protein. The obtained intensity value from control cells was set to 1. Mean (±SD) is shown; n(P-Thr172-P-AMPK) = 3; n(P-Ser239-VASP) = 4; *p < 0.05 (paired t test).

(E) Representative force maps of U2OS cells grown on either 26-kPa or 4-kPa PAA dishes in the absence and presence of CaMKK2 inhibitor (5 μM STO-607 in DMSO). Control cells were treated with DMSO alone.

starvation and is thus expected to exist predominantly in an inactive state in cells grown in rich, serum-containing medium (Hardie et al., 2016). Recent studies provided evidence that AMPK is also linked to mechanosensitive pathways in various cell types. In osteosarcoma cells, AMPK controls mechanosensitive actin filament assembly at focal adhesions through phosphorylating VASP (Tojkander et al., 2015). In epithelial cells, AMPK can be activated in response to the force applied to E-cadherin in a manner that is dependent on its upstream kinase Lkb1 (Bays et al., 2017).

Here, we show that, at least in osteosarcoma cells, CaMKK2 is a critical upstream regulator of mechanosensitive AMPK activation and an important component controlling stress fiber assembly and contractility. During stress fiber maturation, elevated myosin-II-dependent contractility results in tensile forces applied to the focal adhesions located at both ends of the actomyosin bundle. This leads to inhibition of vectorial actin polymerization at focal adhesions through phosphorylation of VASP (Tojkander et al., 2015). We provide evidence that the tensile forces, applied by the contractile stress fiber to the focal adhesions located at its ends, result in local Ca^{2+} influxes, which in turn lead to activation of CaMKK2 at focal adhesions. CaMKK2 subsequently catalyzes local phosphorylation of AMPK in focal adhesions and hence inhibits vectorial actin polymerization through phosphorylation of VASP (Figure 4E). It is important to note that AMPK regulates also other actin-associated proteins, such as actin depolymerizing factor (ADF)/cofilins and myosin regulatory light chain (Banko et al., 2011; Thaiparambil et al., 2012; Schubert et al., 2017). Moreover, AMPK negatively regulates expression of tensins, which control integrin turnover (Georgiadou et al., 2017). Thus, in addition to VASP, CaMKK2 and AMPK may control stress fiber organization and contractility also through other downstream proteins.

CaMKK2 and its downstream kinases, CaMKI, CaMKIV, and AMPK have well-established roles in energy homeostasis, nutrient responses, and cell growth (Marcelo et al., 2016). Furthermore, CaMKK2 is upregulated in multiple tumor types, and its inhibition reduces cell proliferation and tumorigenicity *in vivo* (Lin et al., 2015; Jin et al., 2018). Our work reveals that, in addition to receptors for circulating factors, such as hormones and metabolites (Swulius and Waxham, 2008; Marcelo et al., 2016), also mechanical stimuli can activate CaMKK2 in cells. Thus, CaMKK2 functions as a sensor of both chemical signals and mechanical environment of the cell, and these two functions may be interconnected in the complex tissue environment of multicellular organisms.

Earlier studies demonstrated that stretching of stress fibers evokes local Ca^{2+} influxes near focal adhesions in endothelial cells (Hayakawa et al., 2008). Our results provide evidence that, in osteosarcoma cells, CaMKK2 is activated by local Ca^{2+} influxes in focal adhesions located at the ends of contractile stress fibers. In support to this hypothesis, treatment of U2OS cells with an inhibitor against mechanosensitive ion channels

(F) Quantification of cell-exerted traction forces of control and CaMKK2-inhibited cells on either 26- or 4-kPa dishes. Mean (±SEM) is shown; n(ctrl, 26 kPa) = 28; n(STO-609, 26 kPa) = 31; n(ctrl, 4 kPa) = 8; n(STO-609, 4 kPa) = 7; ***p < 0.001 (Mann-Whitney-Wilcoxon rank-sum test).
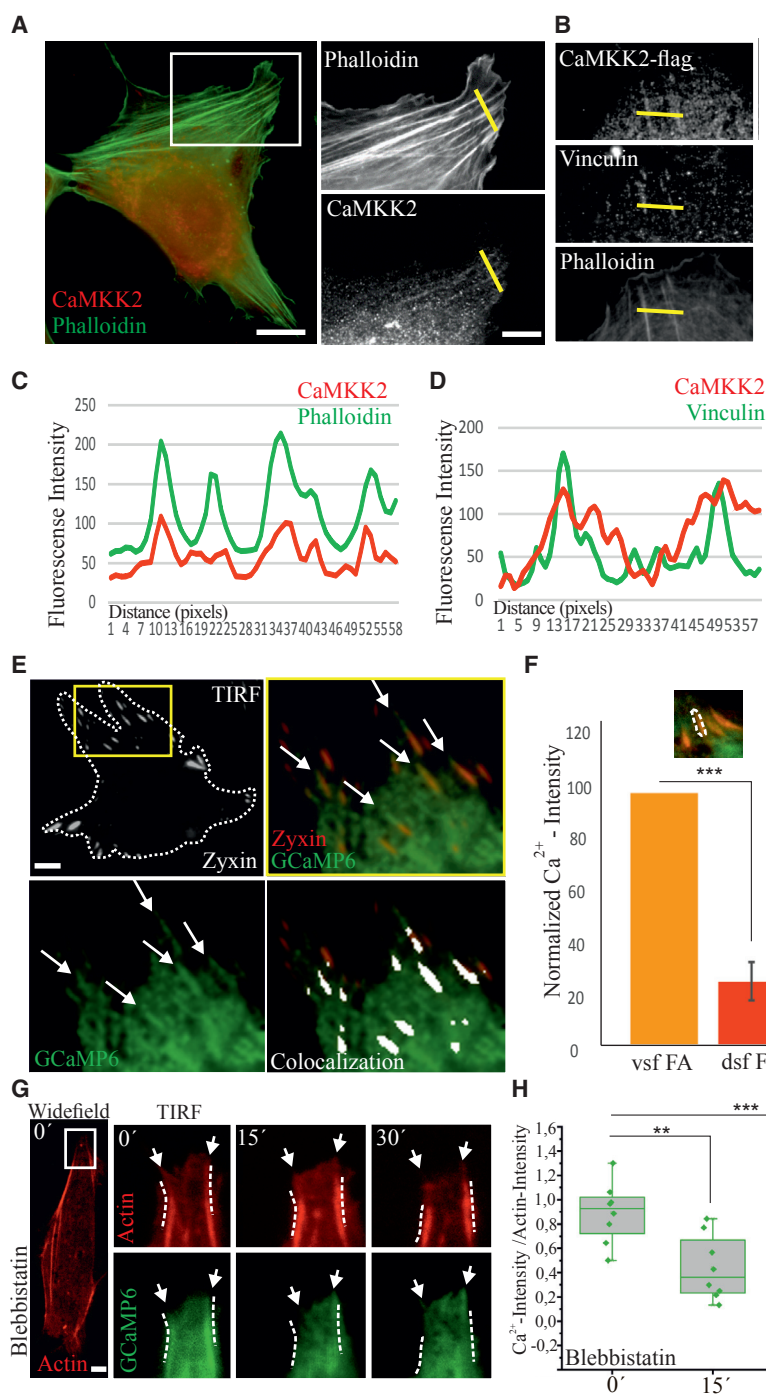
Figure 3. CaMKK2 Is Enriched at Focal Adhesions

(A) U2OS cells stained with Alexa-647-phalloidin to visualize F-actin and with a specific antibody to detect endogenous CaMKK2. The scale bar represents 10 μm.

(B) U2OS cells transfected with a construct expressing CaMKK2-flag. Localization of flag-tagged CaMKK2 was detected with an anti-flag antibody, and focal adhesions and F-actin were visualized by an anti-vinculin antibody and Alexa-488-phalloidin, respectively. The scale bar represents 10 μm.

(C) Line profiles along the yellow line in (A), demonstrating the colocalization of endogenous CaMKK2 and F-actin at the ends of ventral stress fibers.

(D) Line profiles along the yellow lines in (B), demonstrating the localization of CaMKK2-flag to the vinculin-rich focal adhesions.

(E) U2OS cells transfected with a Ca^{2+} indicator GCaMP6 and a plasmid expressing focal adhesion marker mCherry-zyxin. Cells were imaged with TIRF microscopy to reveal the Ca^{2+} signal at the cell-substrate surface. Colocalization was analyzed with ImageJ colocalization finder plugin and is shown as white regions in the bottom right panel. The scale bar represents 10 μm.

(F) Quantification of the Ca^{2+} signal at focal adhesions (FAs) located in the ends of non-contractile dorsal stress fibers (dsf FAs) or contractile ventral stress fibers (vsf FAs). Example of a region of interest (ROI) is shown above the graph. n(dsf FAs) = 14; n(vsf FAs) = 14. Intensities of Ca^{2+} at focal adhesions in the ends of ventral stress fibers were normalized to 1, and mean ± SEM is shown for focal adhesions located in the ends dorsal stress fibers; ***p < 0.001 (paired t test).

(G) Ca^{2+} signal (GCaMP6) at the ends of contractile ventral stress fibers (mCherry-actin) was followed in time after application of 10 μM blebbistatin. Representative frames from TIRF videos taken every 15 min are shown in the panel. White box on the wide-field image indicates the region that is shown in the magnification. White arrows indicate the ends of ventral stress fibers prior to application of blebbistatin. White dashed lines next to the ends of contractile bundles visualize the region that was used for analyses of the data in (H). The scale bar represents 10 μm.

(H) Quantification of the Ca^{2+} signals at the ends of ventral stress fibers at time points 0', 15', and 30' after addition of 10 μM blebbistatin. Intensity of GCaMP6 signal was divided with the intensity of mCherry-actin at the indicated regions (see G).

Raw data, without normalization, were utilized in the analyses. Data are presented in box plots, where the median is indicated by the central bar. 5/95 percentile whiskers with outliers are shown; n(cells) = 8; one contractile bundle from each cell was analyzed; **p < 0.005; ***p > 0.001 (Mann-Whitney-Wilcoxon rank-sum test).

diminished VASP and AMPK phosphorylation and prevented the maturation of contractile ventral stress fibers (Figures 4A and 4B). Mechanical forces can activate several ion channels families (Ranade et al., 2015; Liu and Montell, 2015), some of which have been linked to the actin cytoskeleton and focal adhesions (Ko-bayashi and Sokabe, 2010; Tatsumi et al., 2014). For example, transient receptor potential (TRP) family proteins TRPM4, TRPM7, TRPC1, and TRPV4 are associated with cell migration (Nielsen et al., 2014; Cáceres et al., 2015; Mrkonjić et al., 2015) and TRPC1 and TRPV1 with the formation of myofibrils (Formigli
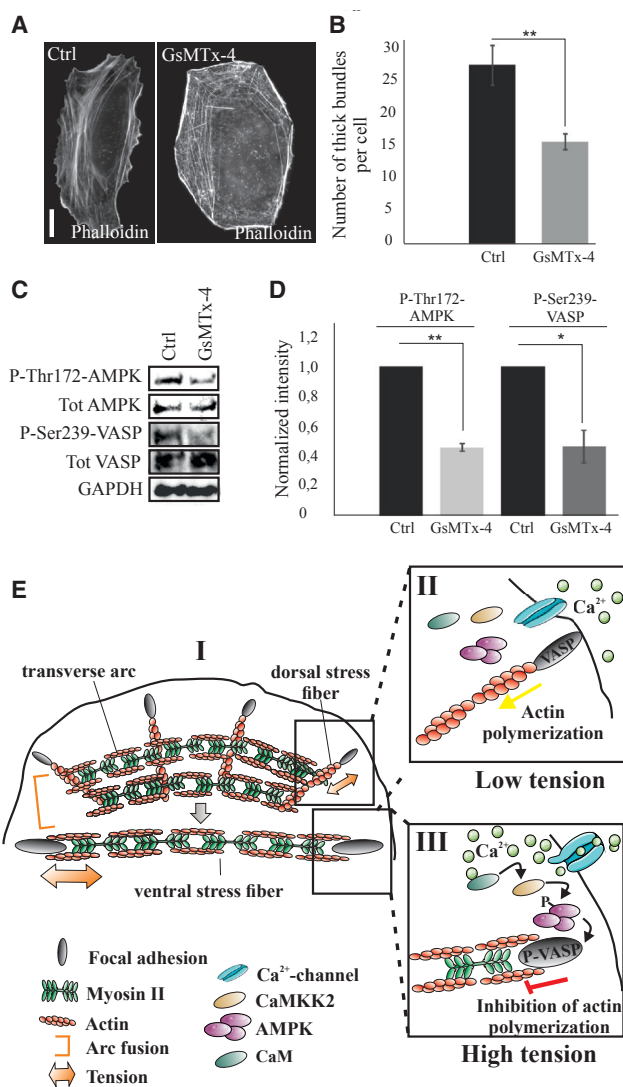
Figure 4. Inhibition of Mechanosensitive Ca^{2+} Channels Leads to the Loss of Mature Stress Fibers

(A) U2OS cells were exposed to 5 μM GsMTx-4 for 6 hr. The actin cytoskeletons were visualized by Alexa-488-phalloidin staining, which revealed immature stress fiber network in inhibitor-treated cells. The scale bar represents 10 μm.

(B) Stress fibers from control and GsMTx-4-treated cells were analyzed by Ridge detection plugin of Fiji ImageJ. The threshold was set in a way that only ventral stress fibers and other prominent actin bundles were detected (see Experimental Procedures). The GsMTx-4-treated cells displayed significantly lower amounts of thick actin bundles. Mean ± SEM is shown; n(ctrl) = 11; n(GsMTx-4) = 14; **p < 0.01 (Mann-Whitney-Wilcoxon rank-sum test).

(C) Western blot experiments to detect the levels of P-Thr172-AMPK, P-Ser239-VASP, GAPDH, total VASP, and AMPK from control and GsMTx-4-treated U2OS cell lysates.

(D) Quantification of the western blot experiments. Ratios of P-Thr172 AMPK versus total AMPK as well as P-Ser239-VASP versus total VASP were calculated. Control cell values were set to 1, and GsMTx-4-treatment values were normalized accordingly. Mean ± SEM is shown; n = 3 for both P-Thr172-AMPK/total AMPK and P-Ser239-VASP/total VASP; **p < 0.01; *p < 0.05 (paired t test).

(E) A working model for the functions of CaMKK2, AMPK, and VASP in the mechanosensitive maturation of contractile actomyosin bundles. (I) Migrating cells display a spider-net-like organization of dorsal stress fibers and trans-

et al., 2009; Yang et al., 2013). Thus, TRP channels represent good candidates for proteins that can drive the mechanosensitive Ca^{2+} influx at focal adhesions. Future work on their role in the context of the Ca^{2+}/CaMKK2/AMPK/VASP-dependent signaling pathway may provide interesting, new molecular insights into the interplay between ion channels and mechanosensitive actomyosin bundles in cells.

EXPERIMENTAL PROCEDURES

Cell Culture

U2OS cells were cultured as in Tojkander et al. (2015) and plated on dishes one day prior to experiments. Treatments of cell cultures is as follows: for CaMKK2 inhibitor, STO-609 (in DMSO; Sigma-Aldrich) was used in a final concentration of 5 or 10 μM and incubated for 3–6 hr; for AMPK inhibitor compound C (dorsomorphin dihydrochloride, in DMSO; Sigma-Aldrich), final concentration of 5 μM for 5 hr; for Ca^{2+} ionophore (in DMSO; Sigma-Aldrich), final concentrations of 1 and 3 μM for 3 hr; for GsMTx4 (in H$_2$O; Abcam), final concentration of 5 μM for 3–6 hr. Ca^{2+} depletion was performed with 3 hr incubation in a Ca^{2+}-free media (Ca^{2+}-free DMEM; Gibco). For CaMKK2 ON-TARGETplus siRNAs, targeted region, non-coding, open reading frame (ORF), J-004842-08-0002, J-004842-09-0002, and J-004842-10-0002 (Dharmacon) were transfected with Ribojuice siRNA transfection reagent (71115-3; Millipore) according to the manufacturer's instructions and incubated for 4 days prior to imaging, fixation, or preparation of cell lysates. Control cells were always treated with the corresponding solvent alone. mCherry-Zyxin, mCherry-Actin, GFP-Calponin3, GCaMP6s-Ca^{2+}-indicator (Addgene), and pSG5-FLAG-CaMKK2 (FL rat; Addgene) were transfected with Lipofectamine transfection reagent (11668-019; Thermo Fisher Scientific) and incubated for 24 hr before imaging. CaMKK2 wild-type and G87R mutant constructs were a kind gift from Dr. John Scott (O'Brien et al., 2017).

Immunofluorescence Microscopy

All immunofluorescence stainings were performed as in Tojkander et al. (2015). Primary antibodies are as follows: anti-CaMKK2 (SAB1302099 and HPA017389; Sigma-Aldrich), anti-FLAG (F1804; Sigma-Aldrich), anti-P-thr172-AMPK (no. 4188; Cell Signaling Technology); and anti-vinculin antibody (1:50; hVin-1; Sigma, Saint Louis, MO). Secondary antibodies are as follows: Alexa Fluor α-rabbit 488 and α-mouse 568 (Life Technologies). Actin filaments were detected with Alexa 488 and Alexa Fluor 647-phalloidins in 1:200 dilution (Life Technologies) and DNA with DAPI (Life Technologies). All antibodies were diluted according to the manufacturers' instructions. DABCO and Mowiol was used in mounting. Images were acquired with Leica DM6000 upright fluorescence wide-field microscope equipped with Hamamatsu Orca-Flash4.0 V2 sCMOS camera. Colocalizations of CaMKK2, actin, and focal adhesion markers were analyzed from line profiles with ImageJ.

Western Blotting

Cell lysates were prepared, and western blotting was performed as in Tojkander et al. (2015), with the following antibodies: anti-P-thr172-AMPK (no. 4188; Cell Signaling Technology); anti-AMPK (SAB4502329; Sigma);

verse arcs. As transverse arcs flow toward the cell center, they fuse with each other to form thicker and more contractile bundles, called ventral stress fibers. Contractile ventral stress fibers exert much stronger traction forces to focal adhesions compared to non-contractile dorsal stress fibers. (II) Weak traction forces generated by dorsal stress fibers allow vectorial actin polymerization at focal adhesions by keeping VASP in its active, un-phosphorylated state. (III) Strong traction forces exerted by the contractile ventral stress fibers activate mechanosensitive Ca^{2+} channels at focal adhesions. The Ca^{2+} influx results in activation of CaMKK2, consequent phosphorylation and activation of AMPK, and downstream phosphorylation of VASP. This leads to inhibition of vectorial actin filament assembly at focal adhesions and therefore halts stress fiber elongation to ensure its proper contractility and maturation.

anti-AMPK (no. 2532; Cell Signal); anti-P-ser239-VASP (clone 16C2; Millipore); anti-CaMKK2 (SAB1302099 and HPA017389; Sigma-Aldrich); anti-VASP (HPA 005724, Prestige Ab; Atlas Antibodies); mouse anti-GAPDH (G8795, Sigma-Aldrich); and anti-Tubulin ab (clone B-5-1-2; Sigma-Aldrich). All antibodies were diluted according to the manufacturers' instructions. Anti-mouse or -rabbit horseradish peroxidase (HRP)-linked secondary antibodies (Cell Signaling Technology) and Western HRP substrate (Luminata Crescendo; WBLUR0100; Millipore) were used for chemiluminescence detection.

Contractile Function

To measure contractile function, the cells were cultured on fibronectin-(FN-650)-coated, crossbow-shaped micropatterns (CYTOOchips, Grenoble, France) for 4–6 hr and fixed with 4% PFA for 20 min. The actin cytoskeleton was visualized with Alexa 488-phalloidin and nuclei with DAPI. Analysis of contractile function is based on the curvature of the formed thick contractile acto-myosin bundle. Radius of curvature (R) was calculated by using the formula

$$R = \frac{\left(\frac{L}{2}\right)^2 + w^2}{w},$$

where L = length and w = width. All measurements were performed with ImageJ program.

Analysis of Stress Fiber Composition

Fiji ImageJ 1.51 Ridge detection plugin was utilized for detecting thick stress fibers from control, CaMKK2-depleted, and CaMKK2-inhibited cells. The following parameters were applied in ridge detection: line width 29.0; high contrast 230; low contrast 87; Sigma 8.87; lower threshold 0.0; and upper threshold 0.17. Please note that, with these settings, the program tracks ventral stress fibers, prominent arcs, and dorsal stress fibers, as well as cortical actin filament bundles.

Traction Force Microscopy

U2OS cells were plated on elastic collagen-1-coated polyacrylamide (PAA) gel substrates with either 26- or 4-kPa stiffness. Traction force microscopy experiments were performed as in Tojkander et al. (2015) with 3I Marianas imaging system, containing a heated sample chamber (+37°C), controlled CO_2, and 63×/1.2 W C-Apochromat Corr WD = 0.28 M27 objective (3I intelligent Imaging Innovations, Germany). Cell-exerted traction fields were computed by using Fourier Transform Traction Cytometry (Tolić-Nørrelykke et al., 2002; Krishnan et al., 2009). The root-mean-squared magnitudes were derived from the traction fields.

Live-Cell Imaging

All wide-field live-cell imaging experiments were performed with 3I Marianas imaging system as in Tojkander et al. (2015). In TIRF microscopy experiments, the same 3I Marianas imaging setup with a 63×/1.46 Alpha Plan-Apochromat Oil Corr WD = 0.10 M27 objective together with chroma TIRF filter cubes, 488/561 TRF59904 were utilized. Images in time-lapse experiments were acquired every 5 s to visualize focal adhesion-associated Ca^{2+} influx. Further analyses of the video frames and measurement of Ca^{2+} signal at distinct focal adhesions were performed with ImageJ program. ImageJ colocalization finder plugin was utilized to detect the colocalization between GCaMP6 and mCherry-actin or mCherry-zyxin from static image frames, extracted from the live-cell videos. Intensity of Ca^{2+} signal at the dorsal- and ventral-stress-fiber-associated focal adhesions was quantified with ImageJ from an area that was defined based on mCherry-zyxin signal (Figure 3F). Ventral stress fibers were defined based on their association with focal adhesions from their both ends, whereas dorsal stress fibers associate with focal adhesion only through their distal ends. Intensity of Ca^{2+} at ventral-stress-fiber-associated adhesions was normalized to 100, and corresponding values for dorsal stress fiber adhesions (within the same cell) were normalized accordingly. In blebbistatin experiments, cells were imaged every 15 min for 1 hr. Intensity of Ca^{2+} signal in blebbistatin experiments was analyzed from line profiles that were drawn along the ends of contractile bundles in single frames, extracted from the videos. The intensity

of GCaMP6 was measured from the raw data and divided by the intensity of mCherry-actin at the same region.

Statistical Analyses

The statistical differences in western blot analyses, where the control values were set to 1, were assessed using the paired t test in Microsoft Excel 2013. Statistical differences in traction force, contractile function, blebbistatin imaging, and ridge detection experiments are assessed by the Mann-Whitney-Wilcoxon rank-sum test (MWW). Box charts were done with Origin 2018 program (whisker range 5–95, showing outliers), and column charts were done with Microsoft Excel 2013.

SUPPLEMENTAL INFORMATION

Supplemental Information includes four figures and one video and can be found with this article online at https://doi.org/10.1016/j.celrep.2018.06.011.

AUTHOR CONTRIBUTIONS

S.T. and P.L. designed the study and wrote the manuscript. S.T. carried out the majority of the experiments, except for the Ca^{2+} depletion experiments and statistical analyses that were performed by K.C.

DECLARATION OF INTERESTS

The authors declare no competing interests.

REFERENCES

Abbott, M.J., Edelman, A.M., and Turcotte, L.P. (2009). CaMKK is an upstream signal of AMP-activated protein kinase in regulation of substrate metabolism in contracting skeletal muscle. Am. J. Physiol. Regul. Integr. Comp. Physiol. 297, R1724–R1732.

Altarejos, J.Y., Taniguchi, M., Clanachan, A.S., and Lopaschuk, G.D. (2005). Myocardial ischemia differentially regulates LKB1 and an alternate 5'-AMP-activated protein kinase kinase. J. Biol. Chem. 280, 183–190.

Banko, M.R., Allen, J.J., Schaffer, B.E., Wilker, E.W., Tsou, P., White, J.L., Villén, J., Wang, B., Kim, S.R., Sakamoto, K., et al. (2011). Chemical genetic screen for AMPKα2 substrates uncovers a network of proteins involved in mitosis. Mol. Cell 44, 878–892.

Bays, J.L., Campbell, H.K., Heidema, C., Sebbagh, M., and DeMali, K.A. (2017). Linking E-cadherin mechanotransduction to cell metabolism through force-mediated activation of AMPK. Nat. Cell Biol. 19, 724–731.

Benz, P.M., Blume, C., Seifert, S., Wilhelm, S., Waschke, J., Schuh, K., Gertler, F., Münzel, T., and Renné, T. (2009). Differential VASP phosphorylation controls remodeling of the actin cytoskeleton. J. Cell Sci. 122, 3954–3965.

Bonini, M.G., and Gantner, B.N. (2013). The multifaceted activities of AMPK in tumor progression–why the "one size fits all" definition does not fit at all? IUBMB Life 65, 889–896.

Burnette, D.T., Manley, S., Sengupta, P., Sougrat, R., Davidson, M.W., Kachar, B., and Lippincott-Schwartz, J. (2011). A role for actin arcs in the leading-edge advance of migrating cells. Nat. Cell Biol. 13, 371–381.

Burnette, D.T., Shao, L., Ott, C., Pasapera, A.M., Fischer, R.S., Baird, M.A., Der Loughian, C., Delanoe-Ayari, H., Paszek, M.J., Davidson, M.W., et al. (2014). A contractile and counterbalancing adhesion system controls the 3D shape of crawling cells. J. Cell Biol. 205, 83–96.

Burridge, K., and Wittchen, E.S. (2013). The tension mounts: stress fibers as force-generating mechanotransducers. J. Cell Biol. 200, 9–19.

Cáceres, M., Ortiz, L., Recabarren, T., Romero, A., Colombo, A., Leiva-Salcedo, E., Varela, D., Rivas, J., Silva, I., Morales, D., et al. (2015). TRPM4 is a novel component of the adhesome required for focal adhesion disassembly, migration and contractility. PLoS ONE 10, e0130540.

Chrzanowska-Wodnicka, M., and Burridge, K. (1996). Rho-stimulated contractility drives the formation of stress fibers and focal adhesions. J. Cell Biol. 133, 1403–1415.

Discher, D.E., Janmey, P., and Wang, Y.L. (2005). Tissue cells feel and respond to the stiffness of their substrate. Science 310, 1139–1143.

Formigli, L., Sassoli, C., Squecco, R., Bini, F., Martinesi, M., Chellini, F., Luciani, G., Sbrana, F., Zecchi-Orlandini, S., Francini, F., and Meacci, E. (2009). Regulation of transient receptor potential canonical channel 1 (TRPC1) by sphingosine 1-phosphate in C2C12 myoblasts and its relevance for a role of mechanotransduction in skeletal muscle differentiation. J. Cell Sci. 122, 1322–1333.

Georgiadou, M., Lilja, J., Jacquemet, G., Guzmán, C., Rafaeva, M., Alibert, C., Yan, Y., Sahgal, P., Lerche, M., Manneville, J.B., et al. (2017). AMPK negatively regulates tensin-dependent integrin activity. J. Cell Biol. 216, 1107–1121.

Hardie, D.G., Schaffer, B.E., and Brunet, A. (2016). AMPK: an energy-sensing pathway with multiple inputs and outputs. Trends Cell Biol. 26, 190–201.

Hawley, S.A., Boudeau, J., Reid, J.L., Mustard, K.J., Udd, L., Mäkelä, T.P., Alessi, D.R., and Hardie, D.G. (2003). Complexes between the LKB1 tumor suppressor, STRAD alpha/beta and MO25 alpha/beta are upstream kinases in the AMP-activated protein kinase cascade. J. Biol. 2, 28.

Hawley, S.A., Pan, D.A., Mustard, K.J., Ross, L., Bain, J., Edelman, A.M., Frenguelli, B.G., and Hardie, D.G. (2005). Calmodulin-dependent protein kinase kinase-beta is an alternative upstream kinase for AMP-activated protein kinase. Cell Metab. 2, 9–19.

Hayakawa, K., Tatsumi, H., and Sokabe, M. (2008). Actin stress fibers transmit and focus force to activate mechanosensitive channels. J. Cell Sci. 121, 496–503.

Hong, S.P., Momcilovic, M., and Carlson, M. (2005). Function of mammalian LKB1 and Ca2+/calmodulin-dependent protein kinase kinase alpha as Snf1-activating kinases in yeast. J. Biol. Chem. 280, 21804–21809.

Hotulainen, P., and Lappalainen, P. (2006). Stress fibers are generated by two distinct actin assembly mechanisms in motile cells. J. Cell Biol. 173, 383–394.

Hurley, R.L., Anderson, K.A., Franzone, J.M., Kemp, B.E., Means, A.R., and Witters, L.A. (2005). The Ca2+/calmodulin-dependent protein kinase kinases are AMP-activated protein kinase kinases. J. Biol. Chem. 280, 29060–29066.

Jensen, T.E., Rose, A.J., Jørgensen, S.B., Brandt, N., Schjerling, P., Wojtaszewski, J.F., and Richter, E.A. (2007). Possible CaMKK-dependent regulation of AMPK phosphorylation and glucose uptake at the onset of mild tetanic skeletal muscle contraction. Am. J. Physiol. Endocrinol. Metab. 292, E1308–E1317.

Jin, L., Chun, J., Pan, C., Kumar, A., Zhang, G., Ha, Y., Li, D., Alesi, G.N., Kang, Y., Zhou, L., et al. (2018). The PLAG1-GDH1 axis promotes anoikis resistance and tumor metastasis through CamKK2-AMPK signaling in LKB1-deficient lung cancer. Mol. Cell 69, 87–99.e7.

Kassianidou, E., and Kumar, S. (2015). A biomechanical perspective on stress fiber structure and function. Biochim. Biophys. Acta 1853 (11 Pt B), 3065–3074.

Kobayashi, T., and Sokabe, M. (2010). Sensing substrate rigidity by mechanosensitive ion channels with stress fibers and focal adhesions. Curr. Opin. Cell Biol. 22, 669–676.

Krishnan, R., Park, C.Y., Lin, Y.C., Mead, J., Jaspers, R.T., Trepat, X., Lenormand, G., Tambe, D., Smolensky, A.V., Knoll, A.H., et al. (2009). Reinforcement versus fluidization in cytoskeletal mechanoresponsiveness. PLoS ONE 4, e5486.

Lin, F., Marcelo, K.L., Rajapakshe, K., Coarfa, C., Dean, A., Wilganowski, N., Robinson, H., Sevick, E., Bissig, K.D., Goldie, L.C., et al. (2015). The camKK2/camKIV relay is an essential regulator of hepatic cancer. Hepatology 62, 505–520.

Liu, C., and Montell, C. (2015). Forcing open TRP channels: mechanical gating as a unifying activation mechanism. Biochem. Biophys. Res. Commun. 460, 22–25.

Marcelo, K.L., Means, A.R., and York, B. (2016). The Ca(2+)/calmodulin/CaMKK2 axis: nature's metabolic CaMshaft. Trends Endocrinol. Metab. 27, 706–718.

Mrkonjić, S., Garcia-Elias, A., Pardo-Pastor, C., Bazellières, E., Trepat, X., Vriens, J., Ghosh, D., Voets, T., Vicente, R., and Valverde, M.A. (2015). TRPV4 participates in the establishment of trailing adhesions and directional persistence of migrating cells. Pflugers Arch. 467, 2107–2119.

Naumanen, P., Lappalainen, P., and Hotulainen, P. (2008). Mechanisms of actin stress fibre assembly. J. Microsc. 231, 446–454.

Nielsen, N., Lindemann, O., and Schwab, A. (2014). TRP channels and STIM/ORAI proteins: sensors and effectors of cancer and stroma cell migration. Br. J. Pharmacol. 171, 5524–5540.

O'Brien, M.T., Oakhill, J.S., Ling, N.X., Langendorf, C.G., Hoque, A., Dite, T.A., Means, A.R., Kemp, B.E., and Scott, J.W. (2017). Impact of genetic variation on human CaMKK2 regulation by Ca2+-Calmodulin and multisite phosphorylation. Sci. Rep. 7, 43264.

Oakes, P.W., Beckham, Y., Stricker, J., and Gardel, M.L. (2012). Tension is required but not sufficient for focal adhesion maturation without a stress fiber template. J. Cell Biol. 196, 363–374.

Prager-Khoutorsky, M., Lichtenstein, A., Krishnan, R., Rajendran, K., Mayo, A., Kam, Z., Geiger, B., and Bershadsky, A.D. (2011). Fibroblast polarization is a matrix-rigidity-dependent process controlled by focal adhesion mechanosensing. Nat. Cell Biol. 13, 1457–1465.

Racioppi, L., and Means, A.R. (2012). Calcium/calmodulin-dependent protein kinase kinase 2: roles in signaling and pathophysiology. J. Biol. Chem. 287, 31658–31665.

Ranade, S.S., Syeda, R., and Patapoutian, A. (2015). Mechanically activated ion channels. Neuron 87, 1162–1179.

Ridley, A.J. (2015). Rho GTPase signalling in cell migration. Curr. Opin. Cell Biol. 36, 103–112.

Ridley, A.J., and Hall, A. (1994). Signal transduction pathways regulating Rho-mediated stress fibre formation: requirement for a tyrosine kinase. EMBO J. 13, 2600–2610.

Schubert, K.M., Qiu, J., Blodow, S., Wiedenmann, M., Lubomirov, L.T., Pfitzer, G., Pohl, U., and Schneider, H. (2017). The AMP-related kinase (AMPK) induces Ca^{2+}-independent dilation of resistance arteries by interfering with actin filament formation. Circ. Res. 121, 149–161.

Shaw, R.J., Kosmatka, M., Bardeesy, N., Hurley, R.L., Witters, L.A., DePinho, R.A., and Cantley, L.C. (2004). The tumor suppressor LKB1 kinase directly activates AMP-activated kinase and regulates apoptosis in response to energy stress. Proc. Natl. Acad. Sci. USA 101, 3329–3335.

Small, J.V., Rottner, K., Kaverina, I., and Anderson, K.I. (1998). Assembling an actin cytoskeleton for cell attachment and movement. Biochim. Biophys. Acta 1404, 271–281.

Soiné, J.R., Brand, C.A., Stricker, J., Oakes, P.W., Gardel, M.L., and Schwarz, U.S. (2015). Model-based traction force microscopy reveals differential tension in cellular actin bundles. PLoS Comput. Biol. 11, e1004076.

Sugimoto, A., Miyazaki, A., Kawarabayashi, K., Shono, M., Akazawa, Y., Hasegawa, T., Ueda-Yamaguchi, K., Kitamura, T., Yoshizaki, K., Fukumoto, S., and Iwamoto, T. (2017). Piezo type mechanosensitive ion channel component 1 functions as a regulator of the cell fate determination of mesenchymal stem cells. Sci. Rep. 7, 17696.

Swulius, M.T., and Waxham, M.N. (2008). Ca(2+)/calmodulin-dependent protein kinases. Cell. Mol. Life Sci. 65, 2637–2657.

Tatsumi, H., Furuichi, T., Nakano, M., Toyota, M., Hayakawa, K., Sokabe, M., and Iida, H. (2014). Mechanosensitive channels are activated by stress in the actin stress fibres, and could be involved in gravity sensing in plants. Plant Biol. (Stuttg.) 16 (Suppl 1), 18–22.

Tee, Y.H., Shemesh, T., Thiagarajan, V., Hariadi, R.F., Anderson, K.L., Page, C., Volkmann, N., Hanein, D., Sivaramakrishnan, S., Kozlov, M.M., and Bershadsky, A.D. (2015). Cellular chirality arising from the self-organization of the actin cytoskeleton. Nat. Cell Biol. 17, 445–457.

Thaiparambil, J.T., Eggers, C.M., and Marcus, A.I. (2012). AMPK regulates mitotic spindle orientation through phosphorylation of myosin regulatory light chain. Mol. Cell. Biol. 32, 3203–3217.

Tojkander, S., Gateva, G., Schevzov, G., Hotulainen, P., Naumanen, P., Martin, C., Gunning, P.W., and Lappalainen, P. (2011). A molecular pathway for myosin II recruitment to stress fibers. Curr. Biol. 21, 539–550.

Tojkander, S., Gateva, G., and Lappalainen, P. (2012). Actin stress fibers–assembly, dynamics and biological roles. J. Cell Sci. 125, 1855–1864.

Tojkander, S., Gateva, G., Husain, A., Krishnan, R., and Lappalainen, P. (2015). Generation of contractile actomyosin bundles depends on mechanosensitive actin filament assembly and disassembly. eLife 4, e06126.

Tokumitsu, H., Inuzuka, H., Ishikawa, Y., Ikeda, M., Saji, I., and Kobayashi, R. (2002). STO-609, a specific inhibitor of the Ca(2+)/calmodulin-dependent protein kinase kinase. J. Biol. Chem. 277, 15813–15818.

Tolić-Nørrelykke, I.M., Butler, J.P., Chen, J., and Wang, N. (2002). Spatial and temporal traction response in human airway smooth muscle cells. Am. J. Physiol. Cell Physiol. 283, C1254–C1266.

Watanabe, N., Kato, T., Fujita, A., Ishizaki, T., and Narumiya, S. (1999). Cooperation between mDia1 and ROCK in Rho-induced actin reorganization. Nat. Cell Biol. 1, 136–143.

Woods, A., Dickerson, K., Heath, R., Hong, S.P., Momcilovic, M., Johnstone, S.R., Carlson, M., and Carling, D. (2005). Ca2+/calmodulin-dependent protein kinase kinase-beta acts upstream of AMP-activated protein kinase in mammalian cells. Cell Metab. 2, 21–33.

Yang, Y., Wang, Z., Yang, H., Wang, L., Gillespie, S.R., Wolosin, J.M., Bernstein, A.M., and Reinach, P.S. (2013). TRPV1 potentiates TGFβ-induction of corneal myofibroblast development through an oxidative stress-mediated p38-SMAD2 signaling loop. PLoS ONE 8, e77300.